Radio Interferometric Quasi Doppler Bearing Estimation

János Sallai, Péter Völgyesi, Ákos Lédeczi
Institute for Software Integrated Systems
Vanderbilt University
Nashville, TN, USA
{janos.sallai, peter.volgyesi, akos.ledeczi}@vanderbilt.edu

ABSTRACT

The paper introduces a novel technique for the bearing estimation of radio sources that can be used for the precise localization and/or tracking of RF tags such as wireless sensor nodes. It is well known that the bearing to a radio source can be estimated by an array of antennas typically arranged in a circular manner. The method is often referred to as Quasi-Doppler measurement. The disadvantage of the existing method is that the receiver is relatively large because of the multiple antennas (typically 8 or 16) and it is computationally intensive to process the high frequency radio signals. Thus, it cannot be done on small, inexpensive radio tags. Instead, we propose to use the array on the transmitter side utilizing as few as three antennas. We use a radio interferometric technique to transform the useful phase information from the high frequency radio signal to a low frequency signal (< 1 kHz) that can be processed on low-cost hardware. Utilizing three anchors nodes with small antenna arrays, any number of low cost wireless nodes with single antennas can be accurately localized.

Categories and Subject Descriptors

C.2.4 [**Computer-Communications Networks**]: Distributed Systems

General Terms: Experimentation, Theory

Keywords: Sensor Networks, Ranging, Localization

Acknowledgments: This work was supported in part by NSF grant CNS-0721604 and ARO MURI grant W911NF-06-1-0076.

Permission to make digital or hard copies of all or part of this work for personal or classroom use is granted without fee provided that copies are not made or distributed for profit or commercial advantage and that copies bear this notice and the full citation on the first page. To copy otherwise, to republish, to post on servers or to redistribute to lists, requires prior specific permission and/or a fee.
IPSN'09, April 13–16, 2009, San Francisco, California, USA.
Copyright 2009 ACM 978-1-60558-371-6/09/04 ...$5.00.

1. INTRODUCTION

In spite of many years of research, the selection of commercially available localization systems for wireless radio nodes is still limited. For outdoor applications, when the nodes do not need to be very cheap and the accuracy requirements are meter scale, GPS is the best choice. Indoor applications could either use Ultra Wide Band (UWB) radios or rely on Radio Signal Strength (RSS). Texas Instruments licensed and integrated the Location Engine [19] developed at Motorola Research into the CC2431 transceiver chip. The system depends on RSS measurements and anchor nodes at known positions and it can achieve 3 m accuracy. PanGo is a active RFID system using 802.11 [2]. It claims room-level resolution relying on dense access point infrastructure. As these and similar systems illustrate, RSS-based methods have relatively low range and accuracy. Moreover, this is not expected to improve significantly since the dependence of radio propagation on the environment, especially indoors, is so significant that a tiny change can cause large effects in the electromagnetic field due to reflections. UWB-based ranging, on the other hand, depends on Time-of-Flight (ToF) measurements. As such, it relies on high sampling rates and nanosecond-scale timing making the hardware somewhat expensive. However, the precision can be quite high. For example, the Ubisense fine-grained localization system has an accuracy of about 20 cm [20]. Unfortunately, the power of UWB radio transmission is limited by law restricting its maximum range to about 20 m [6].

There are quite a few innovative localization approaches in the literature [21], [10], [17], [16] including radio interferometry [13], [9], [8] pioneered by our group. However, none of these have been transitioned to industry. The main reason might be that each of them works under certain assumptions making it applicable only to a subset of applications. A truly universal solution has not emerged yet. This paper introduces a new approach that is not the ultimate solution either, but it may prove to be a step in the right direction.

The paper is structured as follows. In Section 2, we provide a brief overview of existing RF bearing estimation techniques, and propose a novel method employing a small antenna array as a stationary transmitter to enable simple RF receiver tags to estimate their bearing to it. The proposed method exploits the physical phenomenon that an antenna switching at the transmitter results in an instantaneous phase jump in the signal observed at the receiver due to the changed geometry. The mathematical description of bearing estimation is presented in Section 3. In Section 4, we show that the same phase jump is observed when a radio-interferometric measurement technique is used. Section 5 describes an experimental setup using software defined radios outdoors. Our experimental results show that bearings can indeed be accurately estimated. Section 6 describes our ongoing work in this area, namely, a draft design of an antenna switch, the progress toward a scaled down implementation of the bearing computation algorithm that can run on a mote class device and a localization approach using bearing estimates. We conclude the paper with a summary of our contributions in Section 7.

2. BACKGROUND

It was recently shown that the Doppler shift generated by a slowly moving radio transmitter can be utilized to track its location and velocity [8]. The prototype implementation utilizes Mica2 nodes operating at 430 MHz [3]. A person walking with the transmitter at 1 m/s induces a 1.4 Hz shift, which is impossible to measure on the cc1000 radio chip [3]. However, radio interferometry can be used to transform the high frequency carrier into a low frequency signal [13] that has the same amount of Doppler shift. A second, stationery node is needed that transmits a radio signal a few hundred Hz away from the moving node's frequency. The frequency of the envelop of the generated composite signal (measured as the RSS) equals to the difference of the frequencies of the two transmitters. The Doppler shift also appears in this signal and can be measured accurately enough using the simple, inexpensive hardware. If this shift is measured at multiple receivers at known locations, the position and velocity of the tag can be accurately estimated [8]. However, the technique is not suitable for localizing a stationery network due to the lack of Doppler shifts.

A straightforward extension is to rotate the antenna of the transmitter (or even the entire node) at a constant speed and radius [11] (also developed independently by Chang et al. [4]). To a stationery observer, the signal will have a continuously changing frequency determined by the angular velocity of the transmitter, the radius of the circle, and the distance between the rotating transmitter and the receiver. While it is straightforward to compute the distance given the Doppler shift, the radius and the angular velocity, the result is very sensitive to measurement errors if the distance is larger than a few meters. However, the observed frequency change across multiple receivers provides valuable information on the location of the nodes involved [12].

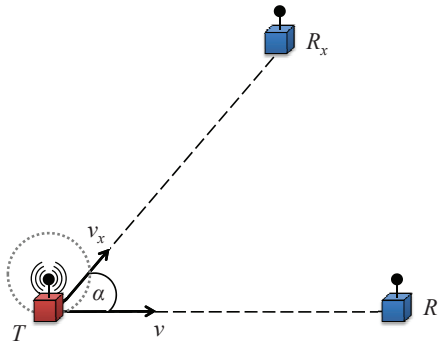

Figure 1: Rotating transmitter

Consider Figure 1. Node T is transmitting a sine wave while rotating its antenna. Simultaneously, receivers R and R_x are measuring the frequency of the received signal. Let us denote the velocity vectors of R and R_x relative to the velocity vector of the rotating transmitter as $\vec{v}$ and $\vec{v}_x$, respectively. From the observed magnitude of both vectors at the point of the maximum frequency shift with respect to receiver R, we get

$$\alpha = \cos^{-1}\left(\frac{|\vec{v}_x|}{|\vec{v}|}\right) \quad (1)$$

where α is the angle $\angle R_x T R$. If T and R are at known positions, we have a bearing estimate to the unknown node R_x. Swapping the roles of T and R then gives us two angles and hence, a location estimate for R_x.

Two factors complicate this approach. First, the generated Doppler shift is tiny compared to the radio frequency. For example, having a Mica2 node rotate at 60 rpm around a circle of 15 cm radius using 430 MHz transmit frequency produces approximately 1 Hz maximum frequency change. This is impossible to measure directly on a receiver mote, but the radio interferometric technique can solve the problem as was shown by Kusy et al. [8]. The other problem is the short-term stability of the crystal oscillator used to generate the RF signal. In our experience, the radio frequency can change several Hz in one second effectively hiding the Doppler shift. The solution we proposed takes the difference of the measured frequencies at the two receivers eliminating the problem [12]. However, equation 1 is not applicable since the ratio of the two relative speeds is no longer available; only their difference is. A somewhat

more complicated approximate solution still produces good bearing estimates [12].

A corresponding application scenario would utilize 3 or more anchor nodes typically surrounding an area where statically deployed and/or mobile RF tags (e.g. wireless sensor nodes) are located. The anchor nodes rotate their antennas one by one according to a schedule and the RF tags and the remaining anchor nodes measure the generated Doppler shift. Then the anchor nodes broadcast their own measurements and positions to the network and in turn, each node would compute its own location. The whole procedure would take a couple of minutes.

This scenario is indeed feasible, but has a significant drawback. The need to rotate the antennas or nodes makes the setup more complicated, more power hungry, more expensive and less robust. These are exactly the design parameters that one tries to optimize in wireless sensor network applications, for example. How can we eliminate the rotation from this scenario?

The effect of rotation is that the physical location of the antenna changes over time causing a phase change at a stationary observer due to the different geometry. The transmit frequency does not change at all, but the continually changing phase causes an apparent frequency change. The observable frequency is a continuous signal due to the rotating motion, but the receiver makes it discrete by sampling it at a certain rate. To be exact, the receiver samples the RF signal and then computes its frequency. Then, if the receiver creates N samples of the frequency signal corresponding to a single rotation, conceptually an identical signal could be constructed by having N antennas arranged uniformly in a circular array. At any one time exactly one antenna transmits. The active antenna is switched around the circle as shown in Figure 2. The observed RF signal will be different from the rotating case since it will have a constant frequency, but sudden phase jumps will appear corresponding to each antenna switch. By measuring these discrete phase changes, N samples of the virtual frequency signal corresponding to the rotating case can be computed.

In addition to eliminating the need for rotation and its corresponding drawbacks, the approach has some significant additional advantages. Switching the antennas can be much faster then physical rotation limited only by the transients in the RF signal and the signal processing approach measuring the phase jumps. Hence, many cycles can be averaged to increase the SNR. The short-term stability of the transmit frequency does not affect the precision since we rely on measuring a nearly instantaneous phase jump eliminating the need to take the difference of the measured frequencies at two receivers. Moreover, the orientation of each antenna array

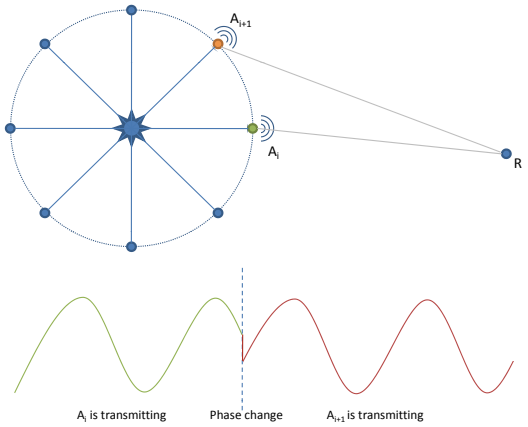

Figure 2: Switched antenna array

can be measured by another anchor node at known position once at deployment time. If the to be localized RF tags get the location and orientation of the anchor nodes at deployment time, they can localize/track themselves without any further communication. Finally, we have exactly N samples per cycle regardless of noise or imprecise/instable sampling rate. That is, the ratio of the fundamental frequency of the frequency signal and the sampling rate is constant and known exactly. This can be utilized effectively in the signal processing approach. Our initial results indicate that as few as 3 antennas provide unambiguous, accurate bearing estimates.

It is well known that antennas positioned less than a wavelength apart exhibit mutual coupling. That is, a transmission from one antenna will induce a current in the other(s), which, in turn, will re-radiate (reflect) the signal. The effective signal emitted from the array will be the superposition of the original and the reflected signals. Since superposition distorts the phase of the compound signal, phase jumps measured at the receiver would also be adversely affected. Instead of calibrating for mutual coupling, we propose a mutually perpendicular arrangement of monopole antennas to avoid it altogether. This way, transmission of one antenna will not induce current in other(s), therefore mutual coupling will not happen. Note that while perpendicular arrangement has previously been used in the literature in order to provide localization capabilities along different perpendicular axes [16], our solution uses it exclusively for mitigating parasitic antenna effects.

It is well known that the bearing to a radio source can be estimated by an array of antennas typically arranged in a circular manner in such a way that the distance between the antennas are smaller than the wavelength of the radio signal. The method is often referred to as Quasi-Doppler (QD) measurement. The disadvantage of the existing method is that the receiver is relatively

large because of the multiple antennas (typically 8 or 16). Also, it is computationally intensive the process the high frequency radio signals especially since it needs to be done on all channels simultaneously. Thus, it cannot be done on small, inexpensive radio tags. Our approach turns the traditional Quasi-Doppler technique around utilizing the antenna array on the transmitter side. This makes it possible to obtain bearing information using a single antenna. When augmented with the radio interferometric technique, the low frequency beat signal (with instantaneous phase jumps) can be observed with mote class devices.

The approach is somewhat similar to the aircraft radio navigation system, VHF Omni-directional Radio Range (VOR) developed in the 1960s and still being used today [1]. The VOR system uses two 30 Hz signals: a frequency modulated omnidirectional reference signal and a rotating directional signal (originally mechanically rotated, but today using an antenna array) which is perceived as an amplitude modulated signal at the receiver. A variant of the system uses the Doppler effect and applies 50 antennas for the variable phase. While the purpose of VOR is the same, to provide bearing information by transmitting a radio signal using an antenna array, the similarities end there. Our technique transmits an unmodulated fixed frequency signal continuously switching the single active antenna around and there is no reference signal. Furthermore, we rely on radio interferometry to enable very simple, low cost and existing COTS hardware to derive bearing information.

3. BEARING ESTIMATION

The rate of change of the phase of a signal is its fundamental frequency. The receiver measures the phase change when the antenna is switched. This phase change is the definite integral between the two measurement instants of a virtual continuous signal, which is the time-varying frequency of the transmitted signal (or more precisely, the envelope of the interference signal because of the interferometric technique). In effect, the switched antenna mimics a physically rotating single antenna that causes a Doppler shift in the observed frequency, hence the name Quasi-Doppler (QD). See Figure 3.

Assuming that the time-varying frequency signal induced by a rotating antenna is $sin(\omega t)$, which is a very good approximation when the distance between the receiver and the transmitter is large relative to the radius of the rotation, the phase change between the instants t and $t + \Delta t$ can be expressed as

$$\Delta\phi(t, t+\Delta t) = \frac{\int_t^{t+\Delta t} sin(\omega t)dt}{\Delta t} \qquad (2)$$

After computing the integral and simplifying, we get

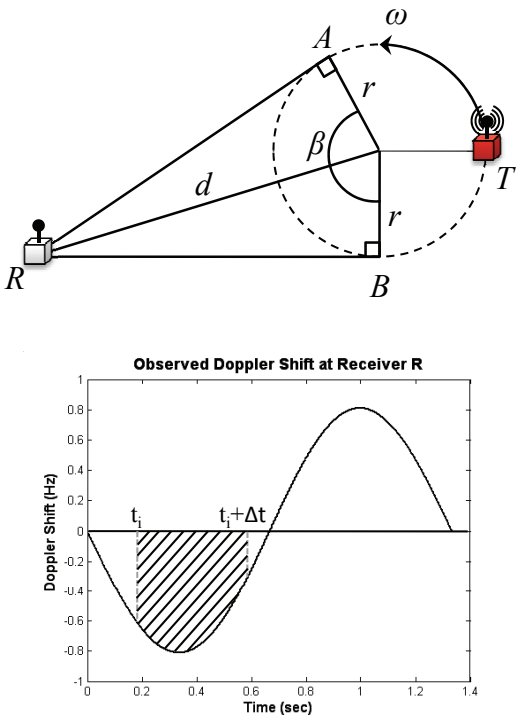

Figure 3: Quasi-Doppler measurement

$$\Delta\phi(t, t+\Delta t) = sin\Big(\omega t + \frac{\Delta t}{2}\Big)\frac{2sin(\frac{\Delta t}{2})}{\omega\Delta t} \qquad (3)$$

This is a sinusoid with frequency identical to the frequency of rotation of the antenna. (Note that $\omega = 1/n\Delta t$, where n is the number of antennas in the array, is an arbitrarily chosen constant in our case.) As long as the Nyquist limit is observed (i.e. with an array of at least three antennas), the virtual time-varying frequency signal of $sin(\omega t)$ can be reconstructed. The phase of this signal, that is, the QD frequency signal, estimated at a receiver gives the bearing to the receiver from the transmitter.

Since both the frequency (ω) and the amplitude—which depends only on ω and the radius of the antenna array—of the frequency signal are known *a priori*, the unknown phase can be estimated by calculating two correlation coefficients between the sampled values and a pair of synthesized sine and cosine signals at the given frequency and amplitude. The arcus tangent of the ratio of these coefficients gives the phase estimate.

A more accurate estimate can be given if several *virtual rotations* are used for calculating the phase of the frequency signal. Since a single rotation consists of a few samples (number of antenna elements), hundreds of rotations can be evaluated even on mote platforms within a second for reducing measurement noise.

4. RADIO INTERFEROMETRY

Since processing high frequency signals on low-power COTS wireless nodes is not feasible, we use a radio-interferometric technique originally introduced by Maroti et al. [13] that allows for measuring the phase shift by analyzing a low frequency beat signal. In addition to the antenna array transmitting a sinusoid of frequency f, an arbitrarily positioned auxiliary antenna is transmitting a sinusoid of frequency $f - f_i$. The superposition of the two signals generates an interference field with beat frequency f_i. Setting the interference frequency to $f_i < 1kHz$ makes it possible to analyze the signal with resource-constrained wireless nodes.

Below we show that a phase change in the high frequency sinusoid results in an equivalent phase change in the beat signal based on the discussion in [13]. We assume that the receiver observes the low-frequency beating using the the received signal strength indicator (RSSI) signal provided by the RF transceiver chip. We model the RSSI signal as the power of the incoming signal mixed down to an intermediate frequency f_{IF}, which goes through a low-pass filter with cut-off frequency f_{cut}, where $f_{cut} << f_{IF}$. Let us assume that the receiver is observing $s(t)$, the superposition of a sinusoid of frequency f, amplitude a_1 and phase φ_1 originating from the transmitter array and a sinusoid of frequency $f - f_i$, amplitude a_2 and phase φ_2 from the auxiliary transmitter:

$$s(t) = a_1 cos(2\pi f t + \varphi_1) + a_2 cos(2\pi(f - f_i)t + \varphi_2)$$

Maroti et al [13] presented the steps to obtain the RSSI signal, which is a sinusoid of frequency 2δ, with a D/C offset:

$$s_{RSSI}(t) = \frac{a_1^2 + a_2^2}{2} + a_1 a_2 cos(4\pi\delta t + \varphi_1 - \varphi_2)$$

From here, it is obvious that when the phase of either high frequency sinusoid component changes, the same amount of phase change will be observed in the observed low-frequency beat signal. Since in our scenario, the phase of the signal originating from the auxiliary transmitter does not change, a phase change in the high-frequency signal from the antenna array will result in an equivalent phase change in the beat signal, observed using the RF transceiver chip's RSSI circuitry.

5. EXPERIMENTAL EVALUATION

We conducted an experiment to verify that the theory does translate to practice, and that it is possible to measure the instantaneous phase jumps corresponding to antenna switchings in a reasonably simple way (i.e. the algorithm can scale down to mote-class hardware). Also, we intended to discover the magnitude and effects of measurement noise, and the limitations the noise poses on the feasibility and precision of bearing estimation. Finally, we used the experimental results to infer some properties of a proposed switched antenna array design (number and arrangement of antennas, switching patterns, etc.) that allows for minimizing non-ideal antenna effects and for mitigating bearing estimation errors resulting from measurement noise.

To minimize environmental disturbances, the experiment was conducted outdoors in an open, rural area.

5.1 Setup

5.1.1 Radio hardware

Although the proposed idea can be implemented on resource constrained devices and does not contain computational intensive algorithms, we made the first experiments with a software defined radio (SDR) platform, the GNU Radio [7]. The use of GNU Radio and the Universal Software Radio Peripheral (USRP) [5] enabled us to generate and/or capture raw radio signals with a bandwidth of up to 8 MHz. This platform also provided a highly flexible framework for experimenting with different signal processing techniques. Furthermore, the USRP frontend provides two (simultaneous) transmit and receive paths, thus simple experiments with a two-antenna array could be made without building an actual antenna switch.

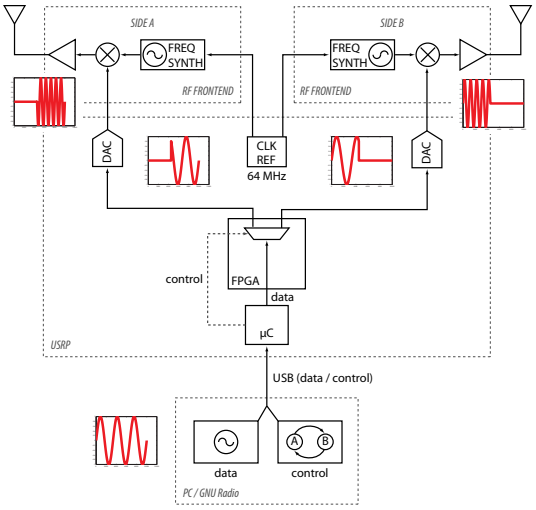

Figure 4: Implementing a transmitter side switched antenna array using Universal Software Radio Peripheral with the RFX400 RF frontend

The USRP component (see Figures 4 and 5) contains up to two (2) analog RF frontend daughtercards, an A/D and D/A converters, an FPGA chip for signal rout-

ing and signal preprocessing and a high speed USB interface controller. Different daughtercards in various frequency bands are supported. We used the RFX400 frontend, which is capable of transmitting and/or receiving quadrature signals in the 400-500 MHz band. These cards are driven by the same reference clock (64 MHz) from the USRP motherboard and synthesize the analog mixer frequency using a fractional PLL with a step size of 4 MHz. The frontends also contain RF amplifiers (LNA, IF filter) and TX/RX switches.

The USRP motherboard contains two CODEC chips—one for each RF frontend—with integrated A/D (64 MSPS, 12 bits) and D/A (128 MSPS, 14 bits) converters. The transmit path of the CODECs also contain digital upconverters driven by fine tuned numerically-controlled oscillators (NCO). These upconverters (up to 32MHz, 2Hz resolution) are used to "augment" the coarse grained tuning of the analog RF frontend boards. Since the CODECs do not provide similar capabilities on the receive path, the on-board FPGA contains digital downconverter cores and decimation filters. The FPGA also contains (de)interleaving logic and a run-time configurable mux/demux pair for routing the logical USB channels to/from the RF frontends.

The transmit and receive channels are interleaved and transferred from and to the PC via the USB interface with an effective bandwidth of 32MB/s. Most of the signal processing is done on the PC using GNU Radio, a generic signal processing framework and a rich set of common signal processing blocks. The blocks are implemented in C++, but the configuration of the signal path is defined in Python scripts. This provides a highly efficient and very flexible environment. The dataflow graph can be (re)configured quite easily using the scripting language, but after the dataflow started, the actual signal processing is carried out by pure C/C++ code.

5.1.2 Transmitter

For experimenting with a switched antenna transmitter, we used two identical daughtercards connected to the same USRP box (Figure 4). The PC side (baseband) synthesized a constant signal with a positive DC offset and periodically reconfigured the signal routing logic (mux) on the FPGA between the two RF frontends. This constant baseband signal creates an unmodulated carrier at the output of the mixer. Since the daughtercards and CODECs are driven by the same reference clock, the two alternative transmit paths use the exact same frequency for mixing. However, the initial phase of the digital upconverters in the CODECs and of the PLLs on the daugthercards are random and cannot be set, thus we had to manually calibrate for approximately zero phase offset at the antennas using an oscilloscope.

Note that for this experiment, we did not use radio interferometry. Since the SDR platform is flexible and powerful enough to carry out the signal processing on the receiver side using the high frequency signal directly, we opted for keeping the setup as simple as possible. Since we experimentally verified the radio inteferometric technique many times in the past under different scenarios [13], [9], [8], we do not expect any unforseen effects when we combine it with the Quasi Doppler technique.

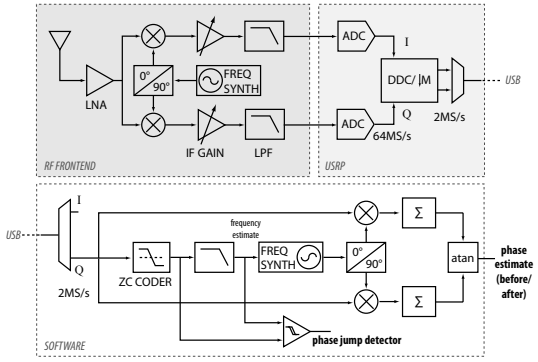

Figure 5: Receiver side signal path using the Universal Software Radio Peripheral with the RFX400 RF frontend

5.1.3 Receiver

The receiver is much simpler on the USRP side (Figure 5). It uses a single frontend card tuned close to the transmitter RF frequency. The PC-based signal processing part receives a low frequency signal with periodic phase changes within the signal. The receiver uses a zero-crossing (ZC) detector and a low-pass filter on the detected period lengths to estimate the frequency of the sinusoid. A phase jump is detected, if the last ZC period significantly deviates from the estimated period length. The receiver then selects two windows—of the same length and separated by an integer multiple of the estimated period length—before and after the period where the phase jump is detected. Then it computes the correlation coefficients between the received signal and a synthesized cosine/sine pair (at the estimated frequency) to calculate the relative phase of the received signal before and after the phase jump.

5.1.4 Configuration

The transmitter pair was placed in the center of a 12m by 12m square, aligned with one of the diagonals. On the transmitter side, we used two monopole antennas arranged perpendicularly to each other (to minimize mutual coupling). The antenna distance was 0.4m.

The experiments were made at 413MHz at low power

levels (few milliwatts). The antenna array was set up to transmit an unmodulated sinusoid at this nominal frequency. However, the real frequency could deviate from this by up to ±50ppm (frequency stability of the reference oscillator). The antenna switching frequency was set to 50Hz.

The receiver, also an USRP device, equipped with a single antenna, was used to measure the phase jumps resulting from antenna switchings at multiple surveyed points on the square. The surveyed points were the vertices, half points and quarter points of the sides of the square. The surveyed points can be seen at angles 0, 18.5, 45, 71.5, 90, 108.5, .., -45, -18.5 degrees, respectively.

The receiver was tuned to receive at 413.001MHz. This means that the RF input received through the antenna is effectively multiplied by a 413.001MHz sinusoid, and is then lowpass filtered with a cutoff frequency of 32MHz. As a result, we expected to see a 1kHz sinusoid as the received signal. The USRP receiver was programmed to sample at 2MHz.

5.2 Results

5.2.1 *Phase jump detection*

The measured periods were typically 950 to 1050 samples long, which corresponds to a received frequency of 2105Hz to 1904Hz at a sampling rate of 2MHz. We observed that the mean period length is slowly changing with time, and the measured period length has a jitter between ±5 samples (±0.5%)in the short term. This can be attributed to two phenomena:

- *Frequency difference of local oscillators from the nominal frequency.* The real crystal frequency mostly depends on temperature and changes slowly with time. Since both the transmitter and the receiver were operating under similar environmental conditions, the observed signal frequency differed only by 1kHz from the expected. As the phase jump detection algorithm uses just a short window of ±10 periods centered around the phase jump, it was safe to assume the period length to be constant.

- *Measurement noise.* There is an additive measurement noise on the received signal, which causes the measured period lengths to fluctuate between ±5 samples around the short-term mean period length. As a result, phase jumps that are equivalent or smaller in magnitude that the noise-related jitter in period length are not possible to detect. Hence, the phase jump detection algorithm has blind spots around bearings of 90 and -90 degrees, where the expected phase jump is close to zero.

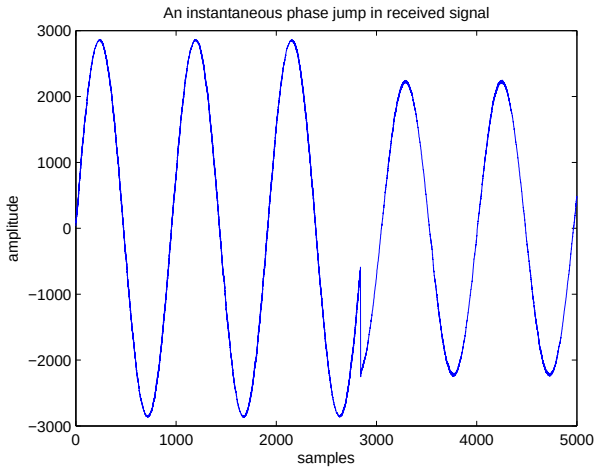

Figure 6: Instantaneous phase jump resulting from an antenna switch measured at a bearing of 71.5 degrees.

Fig. 6 shows a representative measurement, at bearing of 71.5 degrees. The antenna switching is visible in the received signal both as instantaneous phase jump as well as a change in amplitude.

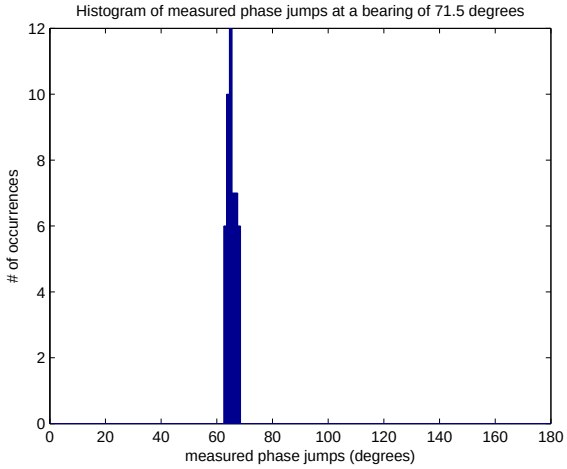

Figure 7: Histogram of consecutive phase jump values measured at a bearing of 71.5 degrees.

Fig. 7 presents the histogram of a series of phase jump values measured at a bearing of 71.5 degrees. The standard deviation is 2.4 degrees, which indicates that consecutive measurements at the same location yield quite consistent phase jump values.

5.2.2 *Phase jump measurements*

We measured a series of phase jumps at every surveyed point. Since the antenna separation was 0.40m, there are some phase jump values that are expected to

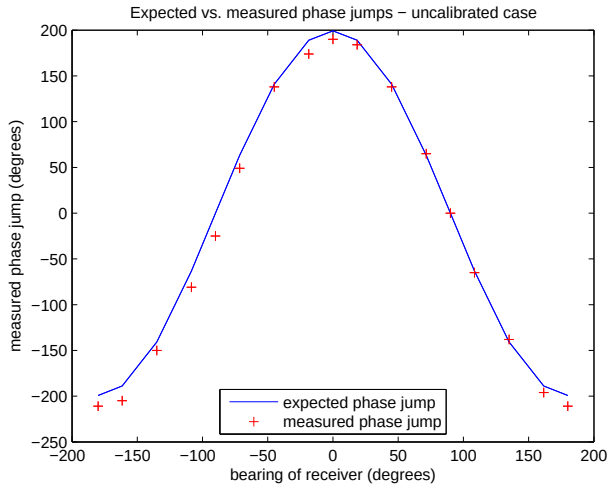

Figure 8: Expected vs. measured phase jumps - uncalibrated case.

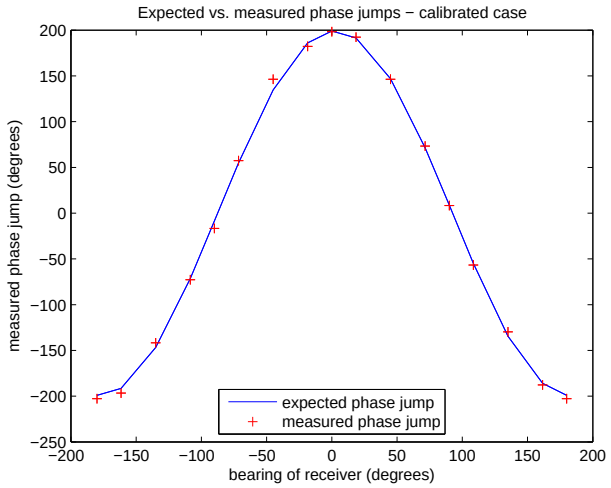

Figure 9: Expected vs. measured phase jumps - calibrated case.

be larger than 180 degrees or less than -180 degrees. The maximum and minimum expected phase jumps are $360\frac{0.40}{\lambda}$ degrees ($\lambda = c/f = 0.72m$), to be expected at bearings of zero and 180 degrees. Since the phase jump measurement algorithm computes values between -180 and 180 degrees, phase jump values that are outside this range become wrapped. In the results presented below, these values are manually unwrapped.

Fig. 8 presents the measured data versus the expected phase jump values. The measured values need to be calibrated for two unknown disturbances:

- *Orientation error of the transmitter array.* The antenna array is placed manually in the center of the surveyed square, parallel to the diagonal of the square. Due to the manual placement, the orientation of the array may be a few degrees off the diagonal.

- *Phase difference of the antennas in the array.* As described earlier, the calibration of the transmitter phases was done manually with an oscilloscope, therefore it may have an error of ± 10 degrees.

Visually, calibration for orientation error involves shifting the measured curve in the the direction of the x axis, while calibration for the phase difference at the transmitter antennas is a shift in the direction of the y axis. Formally, for survey points $i = 1..16$, bearings of survey points θ_i, measured phase jumps $\varphi_{measured,i}$ and expected phase jumps $\varphi_{expected,i}$, where

$$\varphi_{measured,i} = 2\pi \frac{d_{A1,A2}}{\lambda} cos(\theta_i + \mu_\theta) + \mu_\varphi \qquad (4)$$

$$\varphi_{expected,i} = 2\pi \frac{d_{A1,A2}}{\lambda} cos(\theta_i) \qquad (5)$$

we define an objective function $f_{obj,i}$ as

$$f_{obj} = \sum_{i=1}^{16} (\varphi_{expected,i} - \varphi_{measured,i})^2 \qquad (6)$$

which is to be minimized for the bearing error of the transmitter array μ_θ and the phase offset of the transmit antennas μ_φ.

The calibration results for the measured data yielded $\mu_\theta = -2.5$ degrees and $\mu_\varphi = 8.3$ degrees, respectively.

Fig. 9 presents the measured data versus the expected phase jump values after calibrating for the above effects. After calibration, the standard deviation of the measurement errors is 4.7 degrees. Note, however, that the ground truth also has some error as the points were surveyed with a measuring tape on an uneven grassy field.

5.2.3 *Sensitivity of bearing estimation calculation*

Fig. 10 demonstrates the sensitivity of the bearing calculation algorithm to phase jump measurement errors. For each surveyed location between 0 and 180 degrees, we generated a series of phase jump measurements with typical additive Gaussian noise with zero mean and standard deviation of 5 degrees. We calculated the bearing estimates from the noisy phase jump data, and plotted the results in a box plot. As we can see, the bearing estimates become increasingly sensitive to phase measurement noise around 0 and 180 degrees. However, the errors are not amplified by the solver between 18.5 and 161.5 degrees.

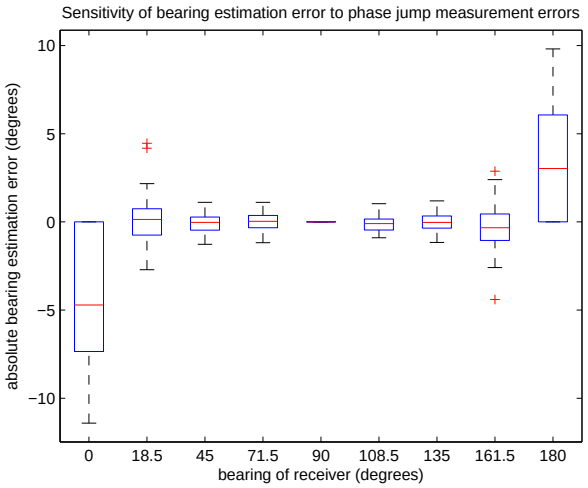

Figure 10: Sensitivity of bearing estimation to phase measurement error

5.3 Evaluation

Based on the experimental results, we can draw the following conclusions:

- *Measurement of instantaneous phase jumps resulting from antenna switchings is feasible.* The above experimental results show that it is possible to measure phase jumps resulting from the alternation of transmit antennas unless the phase jump is less than the phase jitter due to measurement noise, which happens at bearings around 90 and -90 degrees.

- *Phase jump detection and computation scales down to wireless sensor node class devices.* While the above measurements were taken with highly sophisticated radio hardware, this approach can scale down to simple devices with limited processing capabilities.

- *No significant nonideal antenna effects.* With the experimental two-antenna array we could not identify any nonideal antenna effects.

- *Bearing estimation from phase jump measurements is feasible.* We have verified that it is possible to estimate the bearing of a receiver with respect to an antenna array given the assumptions outlined in Section 3. We have observed, however, that at bearings around 0 and 180 degrees, the errors of the bearing estimation are very sensitive to errors in phase jump measurements.

Based on the above findings, an antenna array should have the following properties to be suitable for bearing estimation:

- *Antenna separation.* Distance between antennas between which switchings will occur must be less than $\lambda/2$, where λ is the wavelength of the frequency of the RF signal, in order to avoid wrapping around of phase jump measurements.

- *Spatial diversity of antenna arrangement.* Bearing estimates around ± 90 degrees, as well as around 0 and 180 degrees should be discarded, because of the blind spots of the phase jump measurement and the oversensitivity of the bearing estimation calculation algorithm, respectively. Ideally, the antenna arrangement should be such that if the receiver is in the blind spot/oversensitive region of a pair of antennas, there is at least two other pairs of antennas for which the receiver is outside of their blind spots/oversensitive regions. That is, antenna pairs that lie on lines that are perpendicular should be avoided, since the blind spot of one pair will coincide with the oversensitive region of the other pair, and vice versa. Furthermore, antenna pairs that lie on lines that are parallel should also be avoided, since their blind spots, as well as their oversensitive regions, will coincide. A circular antenna array with an odd number of elements will not suffer from these deficiencies, however, and thus it is a safe choice for our technique.

6. WORK IN PROGRESS

This section highlights three research directions that we are actively working on at the time of publishing of this paper. Our primary goal is to replace the heavyweight software defined radio equipment on both the transmitter and the receiver side with low-power mote-class devices. We envision an asymmetric architecture where the stationary transmitter nodes are equipped with an antenna switch, while the mobile receivers have only single antennas. Below, we present a preliminary design draft of an antenna switch that can be connected to a Mica2 mote. Then, we present the challenges and current status of scaling down the signal processing tasks described in Section 5 to mote class devices. Finally, we provide a brief description on how we envision using bearing estimates for node localization.

6.1 Antenna switch design

Our USRP-based experimental setup for the switched antenna transmitter (see Section 5) enabled two antennas only and added unnecessary complexity to the transmitter side (two complete transmitter frontends instead of just two antennas). For these reasons, having a more suitable transmitter platform is critical in the future development of the presented approach. In the following section, we outline the most important requirements

and potential pitfalls for a switched antenna array to be used for Radio Interferometric Quasi Doppler Bearing Estimation. The block diagram of the antenna switch board we are planning to build is shown in Figure 11.

The antenna switch should completely decouple the switching logic from the transmitter radio (to be able to use the device with almost any RF transmitter). Also, the board should be able to switch between the antennas using arbitrary sequence and timing patterns (e.g., encoding information in the switch time intervals). Thus, the core functionality of the board is implemented by an on-board microcontroller controlling the RF switch/demultiplexer component.

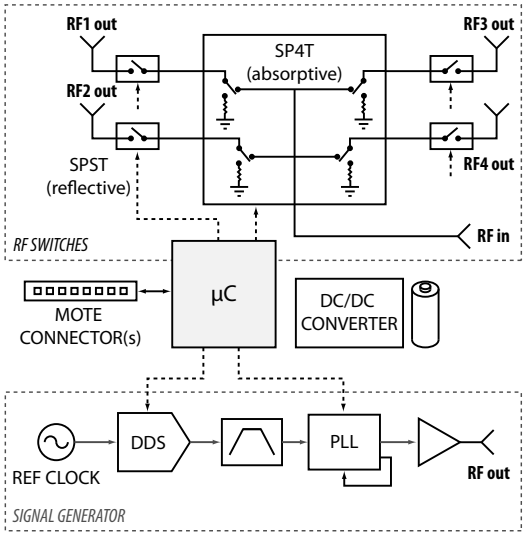

Figure 11: Block diagram of the proposed autonomous antenna switch board

Two prevalent technologies are used to implement the nonlinear element of an RF switch: in PIN diodes, the bias DC current controls the impedance of the diode at RF frequencies, whereas in GaAs FETs, the transistor is fully "on" or "off" depending upon the bias conditions). While PIN diodes are more tolerant against high power RF pulses, GaAs switches offer faster switching time and RF response extending down to DC. For these reasons, GaAs FETs are more suitable in the proposed application. Another important design choice is the termination of the ports in the "off" state. Reflective switch outputs either appear as short or open circuits to the connected antenna element resulting in a very high VSWR (reflection ratio). Absorptive switches present 50 Ω impedance on all outputs/inputs regardless of the switch state. The primary goal when selecting the switch topology in the proposed application is to minimize the effect of the passive (parasitic) antenna elements on the active antenna. Optionally, the performance of the antenna array can be improved by controlling the impedance of the parasitic elements, thereby steering the radiation pattern [18, 15]. To achieve these goals we propose two layers of switches: the initial switch (SP4T or SP8T) being an absorptive component with dedicated SPST reflective switches added to each output. Using this topology one can experiment with and minimize the effects of the different impedance alternatives for the parasitic elements. Due to the bi-directionality of the switch components, the antenna switch board can be used both on the transmitter and/or the receiver sides.

The antenna elements should be connected to the board through flexible coaxial cables to be able to experiment with various antenna spacing and layouts and to keep the size of the board relatively small. For the very same reason, a self-contained power supply solution is preferred. The power requirements of the board are moderate (<10mA @ 3V), a pair of AA-size batteries with a DC/DC converter (3.3V, 5V) is sufficient.

Connectors for existing mote platforms (Mica2, MicaZ, IRIS, Telos) can provide communication channels (I2C, UART) to the on-board microcontroller (e.g., time synchronization between the boards, high-level control interface). They can also provide (consume) power to (from) the connected mote.

Finally, an on-board frequency synthesizer could transform the antenna switching board to a self-contained transmitter node in the proposed application. Martini describes a novel and low-cost approach to implement a highly tunable (200 Hz resolution) wide-band signal generator with low phase noise by utilizing a DDS component as the reference clock for the PLL section of the transceiver [14].

6.2 Receiver implementation

Scaling down the signal processing algorithm that computes the magnitude of the phase jumps observed at the receiver to run on mote class hardware is a challenging task. In our previous work on radio-interferometric tracking [9] we had shown that sampling the RSSI at 8kHz (8-bit samples) is feasible using the Mica2 mote, which leaves approximately 800 clock cycles for processing per each sample. This implies that all processing must be done using fixed point arithmetics in the time domain, and excessive use of multiply-and-sum operations (e.g. long FIR filters) should be avoided.

We are currently experimenting with the following algorithm. First, we remove high-frequency noise from the raw RSSI readings with a moving averager (which is, effectively, a low-pass filter). Keeping a history of samples in a circular buffer, a moving averager can be inexpensively implemented by maintaining an accumulator variable that contains the sum of the samples in the buffer. If the history size is a power of two, the

output of the moving averager can be computed with bitwise shifting of the accumulator, instead of the more expensive integer division.

A switch from one transmit antenna to another, beside resulting in an instantaneous phase jump at the receiver, may also changes the amplitude and the D/C offset of the RSSI signal. To remove the D/C offset, we use a derivator followed by a leaky integrator, which is common practice in digital signal processing. The derivator is essentially a two-tap FIR filter, such that $y[n] = x[n] - x[n-1]$, while the integrator is a one-pole IIR filter, such that $y[n] = \alpha * y[n-1] + x[n]$, where $0 < \alpha < 1$ is the pole. This can be implemented with bitwise shifts instead of multiplication if we choose the pole such that $\alpha = (2^n - 1)/2^n$. Also, to mitigate quantization errors, we represent the integrator's accumulator on 32 bits instead of 8 bits.

Once the D/C offset is removed, we use a simple zero-crossing decoder to find the period lengths, i.e. the sample distance between consecutive negative-to-positive transitions. We store the the period lengths in a buffer.

When the buffer is full, we stop sampling the RSSI and start a task that processes the period lengths offline. Currently, the offline task is searching for sharp changes in period lengths, which indicate an observed phase jump in the received signal. Precisely, 2π times the ratio of the outlier period length and the preceding normal period length gives magnitude of phase jump. From here, we use Equation 5 to compute the bearing.

As of writing this paper, this algorithm performs well on simulated data but falls short in precision when running on noisy RSSI readings acquired by the Mica2 motes. Currently, we are investigating how mitigating measurement noise would be possible with simple signal processing algorithms on mote class devices.

6.3 Localization

One potential application of our bearing estimation technique is node localization. We envision such a system as follows. To localize a node in a plane, two bearings to known locations are necessary. However, it may not be sufficient as the three points may fall in a line. Therefore, we need three anchor nodes with switched antenna arrays at known, not co-linear locations in order to localize nodes. For any one measurement, we need two transmitters: one transmitting using the switched antenna array and one transmitting on a single antenna at a close frequency to create the interference signal. If the antenna array orientation is unknown, then a third node can be used as a receiver to calibrate the orientation of the transmitter. This means that we have three roles for infrastructure nodes in the system. The localization then can proceed as follows (Figure 12). Three

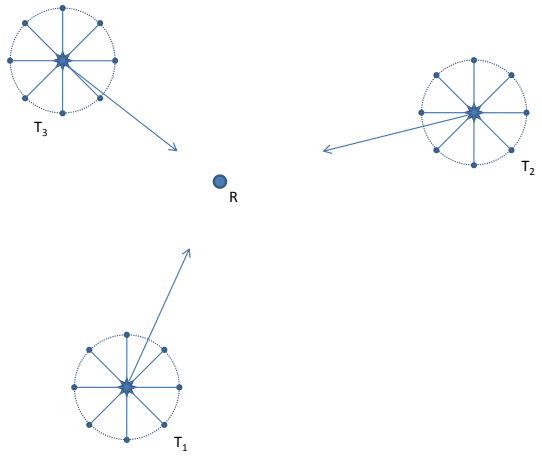

Figure 12: Localization approach

anchor nodes are set up at known locations, but unknown orientation. At initialization time, first one of them (T_1) transmits using the switched antenna array, one (T_2) transmits using a single antenna and the last one (T_3) measures the bearing to T_1. Then they rotate their roles and repeat the measurement. It is enough to perform three such measurements as long as we get a bearing estimate for each node. Since the locations are known, the measured bearings can be easily converted to the orientation of the antenna arrays in the absolute coordinate system. For more accurate results, all six role combinations can be utilized and the resulting two orientation estimates for each node averaged. Once this initialization round is complete, the location and orientation of each anchor nodes are broadcasted to all nodes in the system. Then the anchor nodes start the transmission rounds similar to initialization time according to some schedule. Each node in the system acts as receivers, measure their bearing to the three anchor nodes and compute their own locations.

In our approach, the bearing information is derived from measuring instantaneous phase jumps at a single receiver. Hence, no precise time synchronization is needed between different receivers or between a transmitter and a receiver. However, the receiver still needs to know which antenna is transmitting, i.e., which antenna pair a given phase jump belongs to. Instead of a time synchronization service, however, this can be coded into the transmitted signal itself. Remember that we use the phase jump to reconstruct the (quasi) Doppler-shifted frequency signal. How much time passes between switchings of the subsequent antennas is irrelevant. The only important thing we need to know is that N phase jumps correspond to a full circle, where N is the number of antennas in the array. So, we can use a variable amount of transmission time for each antenna to iden-

tify it. If we have multiple antenna arrays, the same technique can be used to identify the currently active array also. The only requirement is that the transmission time for each antenna in the system needs to be globally unique and distinguishable by the receivers given their clock resolution and accuracy.

7. CONCLUSION

The paper presented a novel idea for bearing estimation in wireless networks and our preliminary work validating it. The unique components of our method are

- Using the switched antenna array on the transmitter side as opposed to the receiver side that is traditional in Quasi-Doppler bearing estimation, so that a single antenna receiver can obtain bearing information.
- Using our radio interferometric technique to transform the useful phase information from the high frequency radio signal (typically >100 MHz) to a low frequency signal (< 1 kHz) that can be processed on low-cost hardware.
- The antenna array can have as few as 3 antennas for unambiguous bearing estimation.
- The proposed antenna switch design can be either a plug-in replacement for a traditional antenna for a mote or SDR, for example, or a standalone transmitter in and of itself.

While there exist challenges before a successful implementation of a full-scale localization service relying on our method will be achieved, the initial results are very promising.

8. REFERENCES

[1] 2001 Federal Radionavigation Systems. http://www.navcen.uscg.gov/pubs/frp2001/FRS2001.pdf.

[2] Pango. `http://www.pangonetworks.com`, 2008.

[3] Chipcon AS, CC1000: Single chip very low power RF transceiver. `http://www.chipcon.com`, 2004.

[4] H.-L. Chang, J.-B. Tian, T.-T. Lai, H.-H. Chu, and P. Huang. Spinning beacons for precise indoor localization. In *Proc. of ACM Sensys*, 2008.

[5] Ettus Research LLC. `http://www.ettus.com`, 2008.

[6] R. Fontana, E. Richley, and J. Barney. Commercialization of an ultra wideband precision asset location system. *Ultra Wideband Systems and Technologies, 2003 IEEE Conference on*, pages 369–373, 16-19 Nov. 2003.

[7] GNU Radio website. `http://gnuradio.org`, 2008.

[8] B. Kusý, A. Lédeczi, and X. Koutsoukos. Tracking mobile nodes using rf doppler shifts. *In Proc. of ACM SenSys*, 2007.

[9] B. Kusý, J. Sallai, G. Balogh, A. Lédeczi, V. Protopopescu, J. Tolliver, F. DeNap, and M. Parang. Radio interferometric tracking of mobile wireless nodes. *In Proc. of MobiSys*, 2007.

[10] Y. Kwon and G. Agha. Passive localization: Large size sensor network localization based on environmental events. In *Proc. of IPSN*, pages 3–14, 2008.

[11] A. Ledeczi, J. Sallai, P. Volgyesi, and R. Thibodeaux. Differential Bearing Estimation for RF Tags. *EURASIP Journal on Embedded Systems (in press)*, 2009.

[12] A. Ledeczi, P. Volgyesi, J. Sallai, and R. Thibodeaux. A novel rf ranging method. *Workshop on Intelligent Solutions in Embedded Systems (WISES 2008)*, July 2008.

[13] M. Maróti, B. Kusý, G. Balogh, P. Völgyesi, A. Nádas, K. Molnár, S. Dóra, and A. Lédeczi. Radio interferometric geolocation. *In Proc. of ACM SenSys*, Nov. 2005.

[14] N. Martini. DIY signal generation. *Circuit Cellar*, (219):12–23, October 2008.

[15] S. Preston and D. Thiel. Direction finding using a switched parasitic antenna array. *Antennas and Propagation Society International Symposium, 1997. IEEE., 1997 Digest*, 2:1024–1027 vol.2, Jul 1997.

[16] K. Römer. The lighthouse location system for smart dust. In *MobiSys*. USENIX, 2003.

[17] R. Stoleru, P. Vicaire, T. He, and J. A. Stankovic. Stardust: a flexible architecture for passive localization in wireless sensor networks. In *Proc. of ACM SenSys*, 2006.

[18] T. Svantesson and M. Wennstrom. High-resolution direction finding using a switched parasitic antenna. *Statistical Signal Processing, 2001. Proceedings of the 11th IEEE Signal Processing Workshop on*, pages 508–511, 2001.

[19] D. Taubenheim, S. Kyperountas, and N. Correal. Distributed radiolocation hardware core for ieee 802.15.4. Technical report, Motorola Labs, Plantation, Florida, 2005.

[20] D. Young, C. Keller, D. Bliss, and K. Forsythe. Ultra-wideband (uwb) transmitter location using time difference of arrival (tdoa) techniques. *Signals, Systems and Computers, 2003. Conference Record of the Thirty-Seventh Asilomar Conference on*, 2:1225–1229 Vol.2, 9-12 Nov. 2003.

[21] Z. Zhong and T. He. Msp: multi-sequence positioning of wireless sensor nodes. In *Proc. of ACM SenSys*, 2007.